







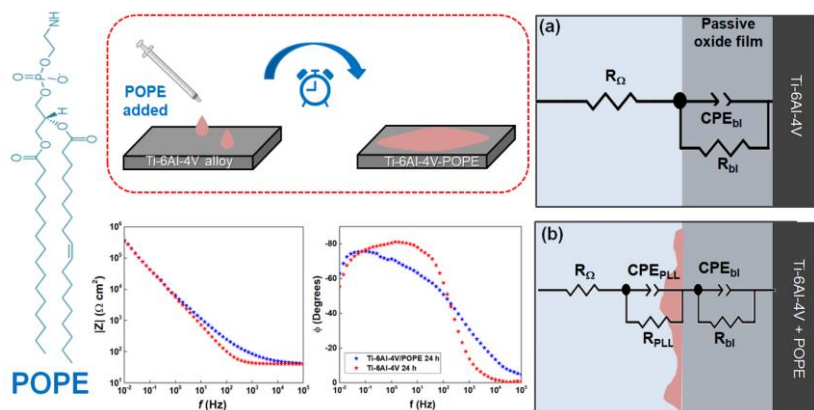
Full Paper | <http://dx.doi.org/10.17807/orbital.v15i5.19304>

The use of POPE Phospholipid as a First-layer Coating of the Ti-6Al-4V Alloy: Preliminary Studies

João Pedro Lopes do Nascimento ^a, Murilo Oliveira Alves Ferreira ^b, Gabriella Teresinha Lima Teixeira ^a, Natália Bueno Leite ^a, Idalina Vieira Aoki ^c, and Jéferson Aparecido Moreto ^b

Phospholipids emerge as a powerful tool to be used as a coating for biomaterials, as they can increase the biocompatibility of the material and inhibit the growth of bacterial cells. Here, POPE phospholipid was deposited on the Ti-6Al-4V alloy surfaces by using a simple method, seeking to improve the corrosion resistance of the base material. Results show that the electrochemical potential of the Ti-6Al-4V/POPE is more positive than that observed in the base material, which could indicate a lower susceptibility to corrosion. Two EECs were used to explain the corrosion mechanisms of the coated and uncoated specimens, demonstrating the base material displays an oxide layer about 1.86 nm in the beginning of the corrosion tests and 2.59 nm after 24 h of immersion. Due to the complexity of the system containing lipids deposited on the metallic matrix, the corrosion behaviour of Ti-6Al-4V/POPE was evaluated considering only the evolution of the CPEs with immersion times. This work shows that the use of POPE for coating the Ti-6Al-4V alloy increased the corrosion resistance of the base material, expanding the range of advantages in the use of this surface treatment in the development of new biomaterials.

Graphical abstract



Keywords

Biomaterials
Coatings
EIS
Phospholipids
Titanium alloy

Article history

Received 23 Aug 2023
Accepted 02 Mar 2024
Available online 01 May 2024

Handling Adilson Beatriz

1. Introduction

As the world population ages and the prevalence of diabetes and other health issues rises, musculoskeletal problems have seen a notable increase. Consequently, the number of individuals afflicted by bone defects due to

osteoporosis, sports injuries, and accidents has grown, posing a considerable threat to human health and overall quality of life [1,2]. In the field of orthopedic and arthroplasty, metallic materials are predominantly employed for implants due to

^a Institute of Exact Sciences, Naturals and Education, Federal University of Triângulo Mineiro (UFTM). Avenida Doutor Randolfo Borges Júnior, Univerdecidade, zip code 38064-200, Uberaba, Minas Gerais, Brazil. ^b Materials Engineering Department, São Carlos School of Engineering, University of São Paulo, zip code 13563-120, São Carlos, São Paulo, Brazil. ^c Polytechnic School, Chemical Engineering Department, University of São Paulo, Av. Prof. Luciano Gualberto, travessa 3, 380, zip code 05508-010, Cidade Universitária, São Paulo, São Paulo, Brazil. *Corresponding author. E-mail: jamoreto@usp.br and natalia.slade@uftm.edu.br

their exceptional mechanical properties, good corrosion resistance in a medium containing aggressive ions as well as biocompatibility. Titanium and its alloys, cobalt-chromium alloys, and stainless-steel stand as the most used metallic biomaterials in the biomedical sector [3,4]. Upon implantation in the host body, the device forms an inert oxide layer, which provides effective protection against corrosive processes. However, this layer hampers bone-implant interaction and fails to yield functional outcomes that match the natural physiological structure [3].

Recent advancements in surface modification techniques aim to discover crucial biological molecular components responsible for cell-cell interaction and adhesion. These components are then replicated on artificial surfaces to promote adhesion points, facilitating cell interactions [5]. As reported by Golub et al [2], the molecular engineering of biocompatible and bioactive surfaces for implantable devices can draw inspiration from biomembranes, which serve as an excellent model [2]. An effective approach involves the use of biomimetic coatings which are composed of phospholipids to enhance the bone-implant contact. Eukaryotic membranes have diverse compositions, with lipids being amphipathic molecules that spontaneously arrange in polar environments. These lipids make up 40% of the cell membrane and have important biophysical properties, contributing to the proper functioning of membrane proteins [6,7] and participating in cell signaling and processes. Studies have shown the potential of using phospholipids as coatings, either as inhibitors of bacterial cells [6], as non-adherent coatings or as coatings for implants that should trigger calcification processes [7].

The phospholipid 1-palmitoyl-2-oleoyl-sn-glycero-3-phosphoethanolamine (POPE), appears as a powerful tool to be used as coating and may be associated to the metallic matrix [5,8,9]. This study introduces a groundbreaking and practical investigation focusing on employing POPE as the initial layer coating for the Ti-6Al-4V alloy. The research evaluates how POPE affects the electrochemical properties of the Ti-6Al-4V alloy by using open-circuit potential (OCP) and electrochemical impedance spectroscopy (EIS) techniques. Additionally, an equivalent electrical circuit (EEC) was proposed to elucidate the electrochemical behaviour of both the coated and uncoated specimens

2. Material and Methods

Ti-6Al-4V alloy was used in the present survey as received condition. Prior the functionalization, all samples were mechanically polished by using SiC sandpapers in the sequence range of 800, 1200, 2400 and 4000#, washed in distilled water, degreased in isopropanol for a period of 10 min and dried. Before the deposition of the lipid thin films, all samples were washed by chloroform during 10 min. After drying, 100 μ L of phospholipid POPE in chloroform (1 mg mL⁻¹) was added to the samples as follows: dropwise, covering the entire surface of the samples with the aid of a syringe. After drying the first layer, the remaining volume was deposited. Subsequently, the coated material was dried with nitrogen gas and placed in a vacuum desiccator for 3 h, where it remained until the beginning of the electrochemical tests.

The corrosion potential (E_{corr}) of the samples was monitored during 1 h to verify the thermodynamic stability of

the coated and uncoated specimens. EIS spectra were obtained using the frequency range of 105 to 10 mHz, an applied a.c. signal of 10 mV (rms), 10 points per decade at increased immersion times of the 3, 6, 9, 12 and 24 h of immersion, respectively. All electrochemical tests were carried out in a naturally aerated 0.6 mol L⁻¹ NaCl solution at room temperature by using a STAT-I-400S potentiostat/galvanostat. The experimental setup followed a classical three-electrode configuration, working electrodes: Ti-6Al-4V and Ti-6Al-4V/POPE with an exposed area of 1 cm², a saturated calomel reference electrode, SCE, (Hg/Hg₂Cl₂/KCl_{sat}), and a platinum as auxiliary electrode. For EIS data fitting, the ZView2 software was used.

3. Results and Discussion

Representative curves of the OCP evolution with the immersion time for the Ti-6Al-4V and Ti-6Al-4V/POPE are presented in **Figure 1**. Results demonstrated that the potential value for the functionalized material is about 55 mV less negative when compared to the bare material (-0.241 V/SCE versus -0.186 V/SCE), indicating a nobler potential and probable lower susceptibility to corrosion process. Considering the base alloy, the potential values determined on the OCP measurements are in line with those displayed in the literature [10]. Furthermore, as mentioned in the literature [11,12], different values of this parameter are expected, since it is dependent on the chemical composition of the solution, pH as well as the temperature of the studied system. **Figure 2** displays the Nyquist diagrams for the Ti-6Al-4V and Ti-6Al-4V/POPE samples. Considering the time 24 h of immersion, the coated specimen exhibits a slightly superior behaviour when compared to the base material. An overall analysis of the Bode spectra (see **Figure 3 (a)**) indicates the bare alloy exhibited a phase angle close to -80°, which may be related to a capacitive behaviour. In other words, a passive film, probably TiO₂, is present on the Ti-6Al-4V alloy surface. With respect to Ti-6Al-4V/POPE (see **Figure 3 (b)**), throughout all the immersion times, the coating's stability in the 0.6 mol L⁻¹ NaCl solution was confirmed.

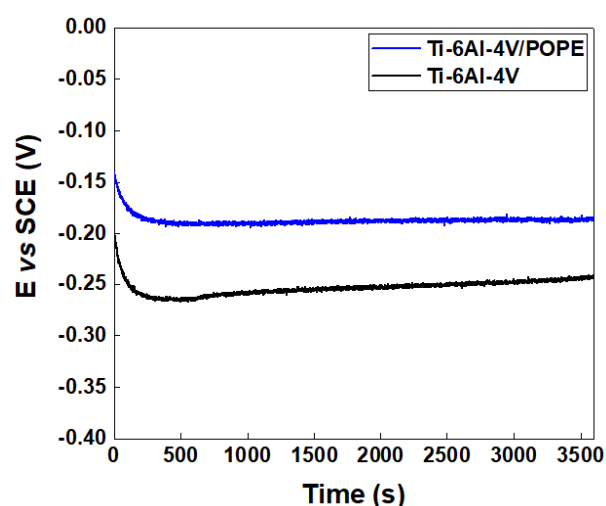


Fig. 1. Open circuit potential variation with time for Ti-6Al-4V and Ti-6Al-4V/POPE in aerated 0.6 mol L⁻¹ NaCl solution.

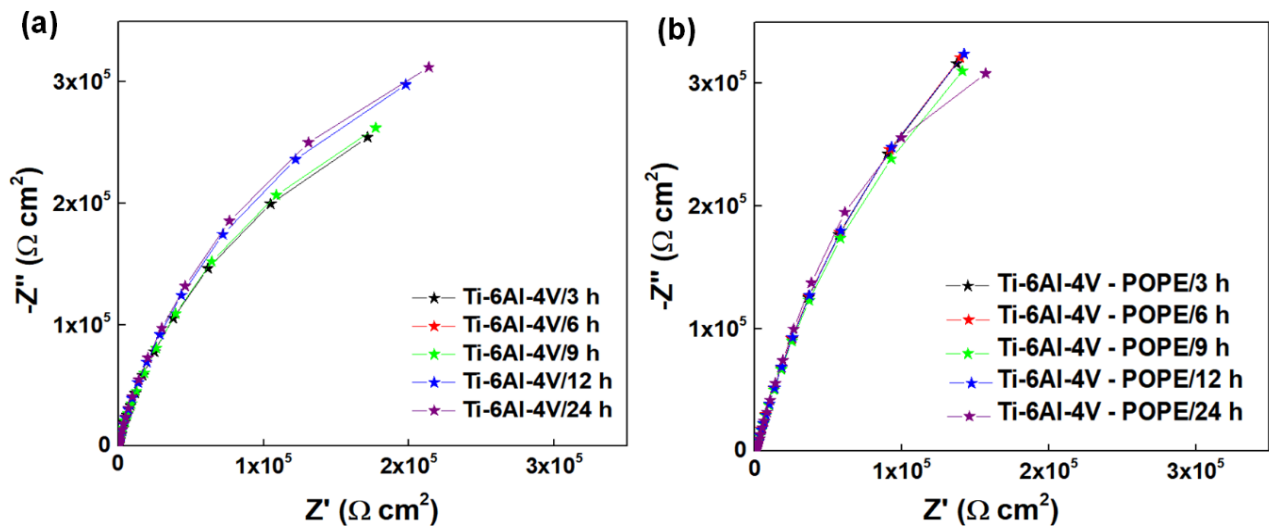


Fig. 2. Nyquist diagrams of Electrochemical Impedance Spectroscopy spectra of Ti-6Al-4V and Ti-6Al-4V/POPE specimens exposed to aerated 0.6 mol L⁻¹ NaCl solution.

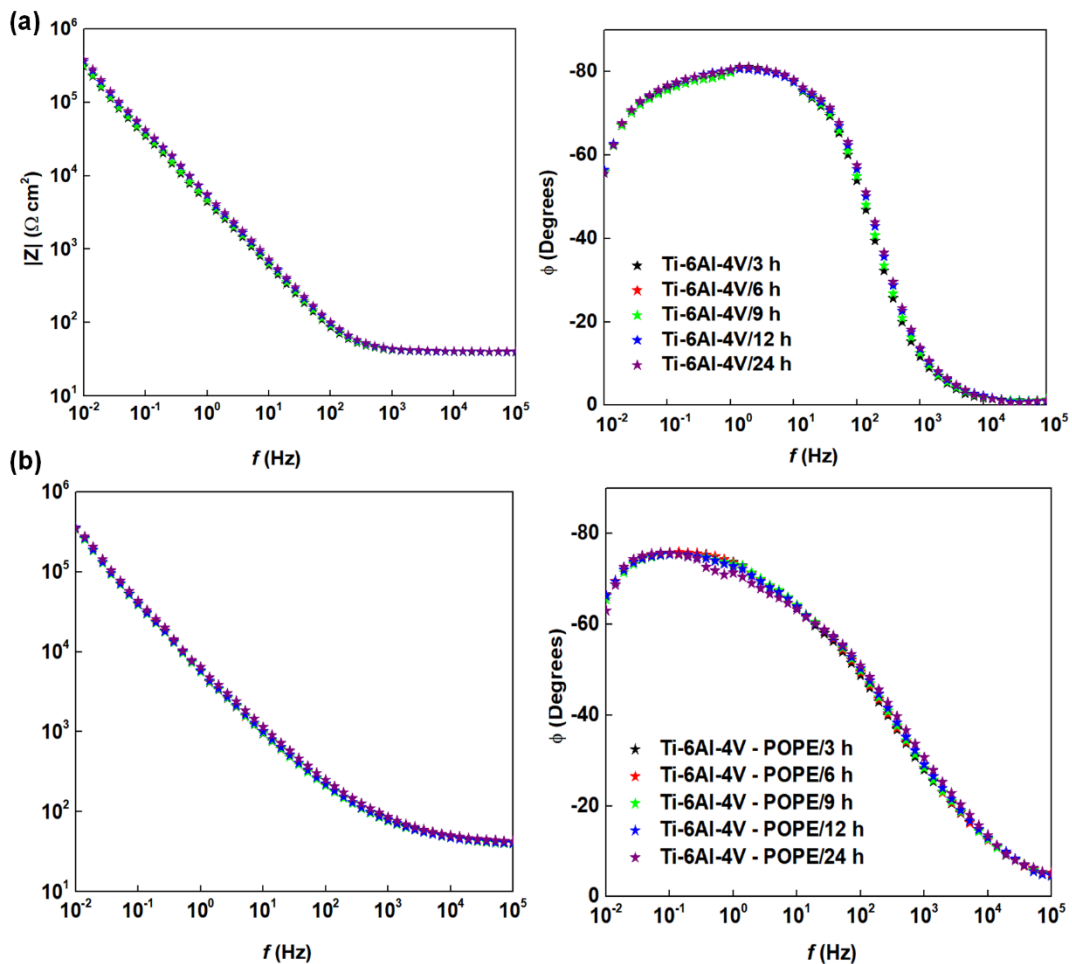


Fig. 3. Bode plots of Electrochemical Impedance Spectroscopy spectra of Ti-6Al-4V and Ti-6Al-4V/POPE specimens exposed to aerated 0.6 mol L⁻¹ NaCl solution.

The electrical equivalent circuits (EECs) depicted in **Figure 4** were proposed to understand the corrosion behaviour of the uncoated and coated specimens. The first one (see **Figure 4 (a)**), named EEC1, was proposed for the base material, and is composed of the Ohmic resistance (R_{Ω}) and the loop $CPE_{bi} - R_{bi}$ that describes the constant phase element of the barrier layer and the resistance of the barrier layer. The second one, named

EEC2, is displayed in **Figure 4 (b)** and was used to describe the corrosion properties of the Ti-6Al-4V/POPE. In this EEC2, the R_{Ω} corresponds to the Ohmic solution resistance, the loop $CPE_{PLL} - R_{PLL}$ is associated with the phospholipid layer (outer layer) and the loop $CPE_{bi} - R_{bi}$ is related to the inner layer. All fittings obtained in this work showed a chi-square (χ^2) of the order of 10^{-4} .

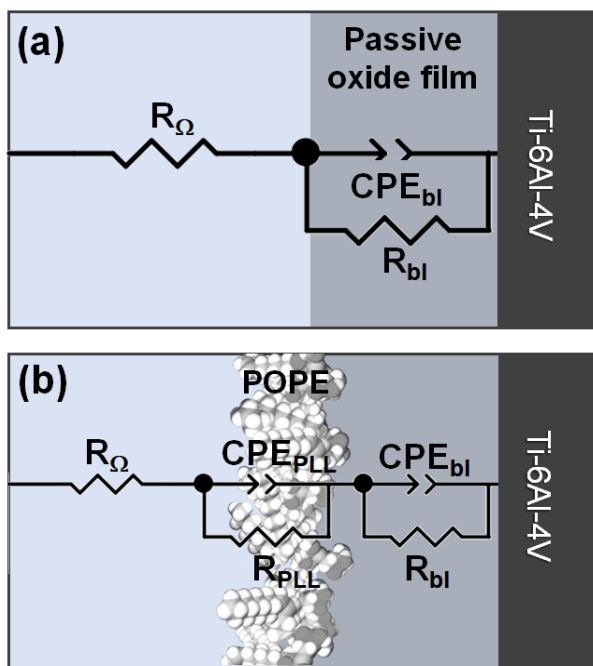


Fig. 4. Schematic representation of the corrosion and the proposed equivalent circuit, (a) Ti-6Al-4V and (b) Ti-6Al-4V/POPE.

The CPE parameter can be used to represent a double layer that presents deviations from an ideal capacitor. The impedance of a CPE (Z_{CPE}) is given by the **Equation 1**:

$$Z_{CPE} = \frac{1}{Y_0 (j\omega)^n}$$

(1)

where Y_0 is a parameter related to capacitance and ϕ is the constant phase exponent, where $0 < n < 1$.

As evident from the results, the R_Ω values remain constant during the immersion tests. This observation, as reported by Moreto et al [13], indicates the distance between the reference and working electrodes throughout all the electrochemical tests is kept constant. The CPE_{bl} values show a decreasing trend with immersion time and the opposite effect was verified for the R_{bl} parameter, as expected. At this time, considering the CPE_{bl} values as capacitance, this increase can be explained by the (i) change in the dielectric constant values (ϵ), (ii) expansion of the electroactive area, and/or (iii) reduction of the oxide thickness on the Ti-6Al-4V alloy surfaces. The presence of roughness and defects on the material's surface leads to a non-uniform current distribution, directly influencing the n values. For the base material, the values of n_{bl} are very close to 0.90, demonstrating a fairly homogeneous surface. **Figure 5** summarizes all results obtained for EEC1.

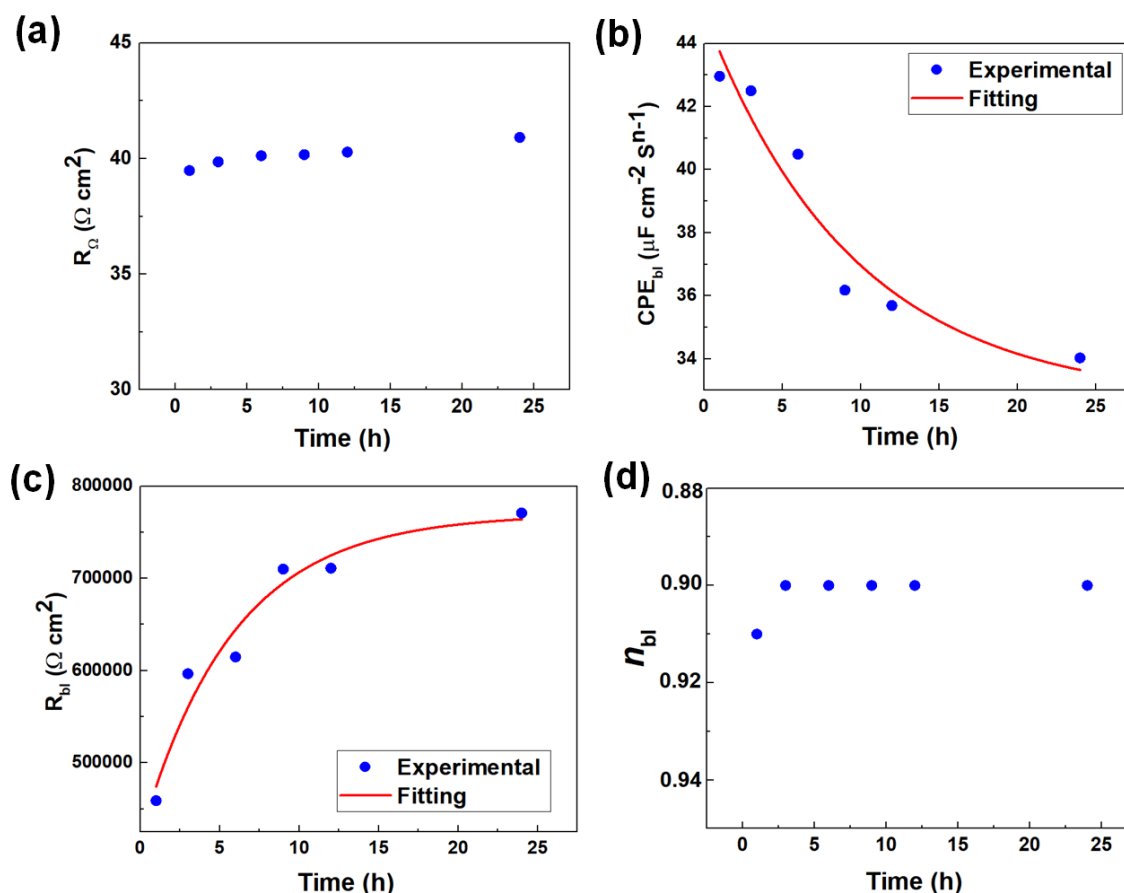


Fig. 5. Evolution with immersion time on the Ti-6Al-4V alloy, (a) R_Ω versus time, (b) CPE_{bl} versus time, (c) R_{bl} versus time, and (d) n_{bl} versus time.

The typical fitting results for the Ti-6Al-4V alloy containing POPE as coating is summarized in **Figure 6**. As can be seen,

the n_{PLL} values obtained for the lipid layer may be related to greater roughness as well as heterogeneity, to the molecular

organization level of the lipids and to the kinetic processes, such as adsorption and phase transitions that occur at the interface [14-16]. As mentioned in the literature [17], values of $n = 0.6 \pm 0.1$ can be assigned to a non-homogeneous 2D or 3D system. Furthermore, the presence of certain ions or electrolyte molecules directly influence the resistivity and dielectric characteristics of lipid phases [180]. On the other hand, the values of n_{bl} are between 0.91 and 0.94, respectively. The values of CPE_{bl} and R_{bl} exhibit very similar behaviour, regardless of the immersion time, suggesting good resistance of the barrier layer against the corrosion process. The

opposite effect was verified for the CPE_{PLL} parameter. In the first six hours of immersion, CPE_{PLL} values are very similar. However, there is a trend towards lower values with immersion time. These observations can be associated with the way in which the phospholipids are organized on the surface of the Ti-6Al-4V alloy. The unsaturations present in the region of the POPE hydrocarbon chains can affect this organization, as they influence the geometry of the lipid and consequently its ordering [19]. Regarding the R_{PLL} parameter, no clear trend was observed.

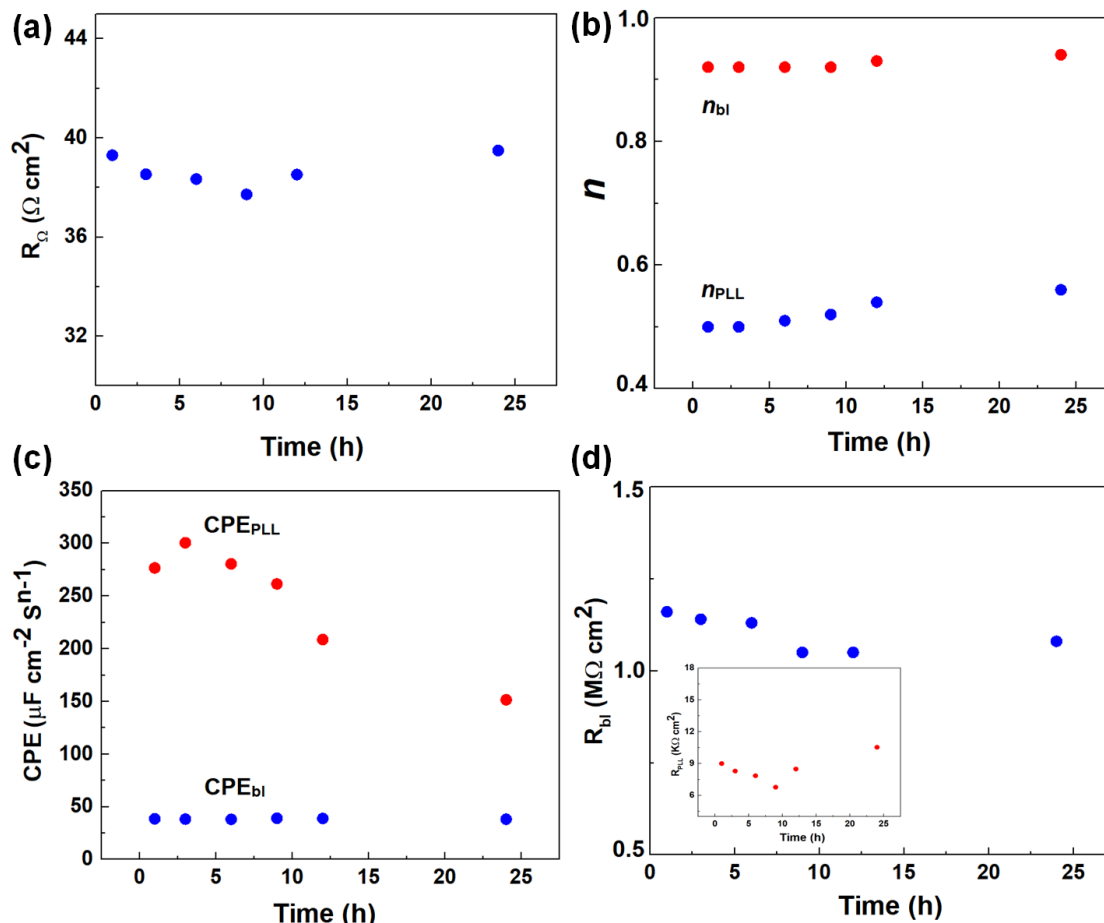


Fig. 6. Evolution with immersion time on the Ti-6Al-4V alloy containing POPE, (a) R_{Ω} versus time, (b) n_{PLL} and n_{bl} versus time, (c) CPE_{PLL} and CPE_{bl} versus time, and (d) R_{bl} versus time. The inset in **Figure 6** (d) represents the R_{PLL} behaviour as function of immersion time.

Here, the CPE_{bl} values were converted to capacitances (C_{bl}) for the Ti-6Al-4V alloy, seeking to determine the thickness of the oxide layer with the evolution of the corrosion process. For this purpose, the **Equation (2)** that was presented by Moreto et al [20] to study the corrosion properties of the 2524-T3 aluminium alloy containing Nb_2O_5 coatings and derived from Brug's equation [21] was used to determine the C_{bl} values. It is important to mention that this relationship can only be used for values of $n > 0.8$.

$$C_{bl} = \left[CPE_{bl} \times R_{\Omega}^{(1-n)} \right]^{\frac{1}{n}} \quad (2)$$

Assuming a parallel plate capacitor, the dependence of the capacitance with thickness is given as:

$$C_{bl} = \frac{\epsilon \epsilon_0 A}{d} \quad (3)$$

where ϵ_0 is the free space permittivity ($8.854 \times 10^{-14} \text{ F cm}^{-1}$), ϵ is the dielectric constant, d the thickness and A represents the area. As mentioned by the literature [22-24], the dielectric constant of the TiO_2 thin film formed on the Ti-6Al-4V alloy displays values between 48 and 100. Thus, from **Equations 3** and **4** it is possible to determine the thickness of the oxide layer on the Ti-6Al-4V alloy surface with the immersion time.

$$d = \frac{\epsilon \epsilon_0 A}{C_{bl}} \quad (4)$$

Figure 7 (a) shows the thickness evolution of the oxide layer on the Ti-6Al-4V alloy surface with immersion time when exposed to 0.6 mol L^{-1} NaCl solution, considering $\epsilon = 48$. **Figure 7** (b) exhibits the influence of the dielectric constant on the thickness of the oxide layer. As can be seen, the thickness at the beginning of the tests is approximately 1.86 nm,

increasing until 24 h of immersion and reaching a value of the order of 2.59 nm. Thus, considering intermediate values between 48 and 100 for the ϵ parameter, the oxide thicknesses obtained in the present work are in line with the literature [25]. So, returning to some previous comments, the increase on the C_{dl} values is directly linked to the ϵ parameter.

And, finally, based on the complexity of the system containing lipids, which may be related to the homogeneity of the POPE distribution along the surface of the Ti-6Al-4V alloy, in the present work the corrosion behaviour was evaluated considering only the evolution of the CPE with immersion times. Although, in general, the POPE-based coating increased the corrosion resistance of the Ti-6Al-4V alloy. This brief communication shows the great potential of POPE phospholipid as a first layer coating and opens up new opportunities for innovative and applied studies in the biomedical sector. Despite this, further studies regarding the structure and morphology of the lipid phase over the Ti-6Al-4V are extremely needed and constitute the next steps by this research group.

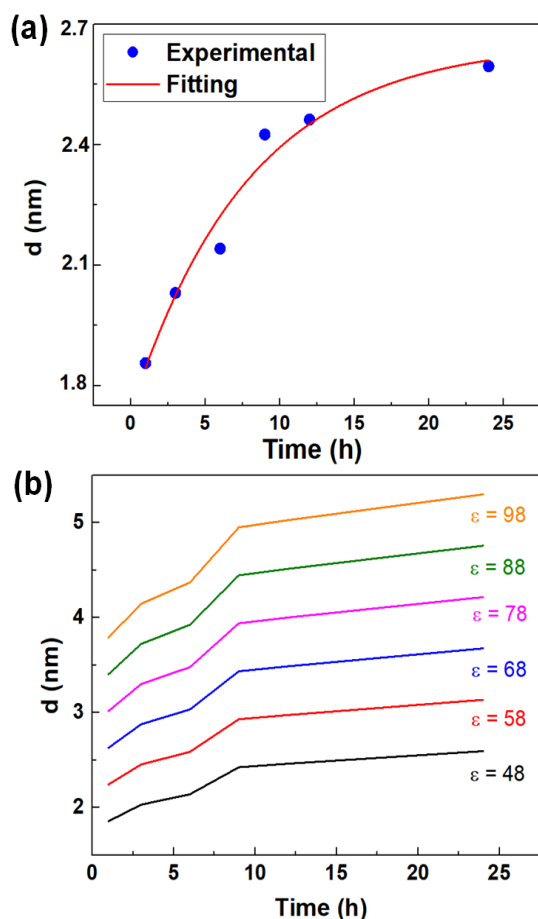


Fig. 7. (a) Thickness evolution of the oxide layer on the Ti-6Al-4V alloy surface with immersion time when exposed to 0.6 mol L⁻¹ NaCl solution, considering $\epsilon = 48$, and (b) influence of the dielectric constant on the thickness of the oxide layer

4. Conclusions

Many efforts have been employed in the treatment of metallic surfaces in search of biocompatible materials. The use of phospholipids for coating metallic alloys has drawn the attention of researchers, as they are versatile and capable of

improving the biofunctional properties of various materials. Despite this, there are few studies that explore the effects of these treatments on the corrosion properties of materials. To fill this gap, we performed POPE deposition on Ti-6Al-4V alloy and performed OCP and EIS techniques to evaluate how POPE affects the electrochemical properties of Ti-6Al-4V alloy. Equivalent electrical circuits were proposed to elucidate the electrochemical behavior of coated and uncoated samples. Overall, the results showed that the presence of POPE imparted higher corrosion resistance to the Ti-6Al-4V alloy, indicating the potential use of this assembled POPE layer to functionalize Ti alloy and other biomedical materials.

Acknowledgments

J. A. Moreto would like to acknowledge the financial support received from the National Council for Scientific and Technological Development (CNPq-Brazil) (Grants 303659/2019-0, 402988/2021-3, 302770/2022-4). N. B. L. Slade would like to acknowledge the financial support received from the Foundation for Research Support of the State of Minas Gerais (FAPEMIG-Brazil) (Process: APQ-00554-21).

Author Contributions

Nascimento, J. P. L. – Investigation; Ferreira, M. O. A. – Investigation; Teixeira, G.T. L. – Investigation; Aoki, I. V. – Formal analysis; Slade, N. B. L. – Project administration, Supervision, Investigation, Formal analysis and writing-up; Moreto, J. A. – Project administration, Supervision, Investigation, Formal analysis and writing-up.

References and Notes

- [1] Chen, X.; Zhou, J.; Qian, Y.; Zhao, L. Z. *Mat. Tod. Bio.* **2023**, *19*, 100586. [\[Crossref\]](#)
- [2] Golub, M.; Lott, D.; Watkins, E. B.; Garamus, V.; Luthringer, B.; Stoemer, M.; Schreyer, A.; Willumet, R. *Biointer.* **2013**, *8*, 21. [\[Crossref\]](#)
- [3] Goriainov, V.; Cook, R.; Latham, J. M.; Dunlop, D. G.; Oreffo, R. O. C. *Acta Biomater.* **2014**, *10*, 4043. [\[Crossref\]](#)
- [4] Anene, F.; Jaafar, C. N. A.; Zainol, I.; Hanim, M. A. A.; Suraya, M. T. *Proc. Inst. Mech. Eng. C. J. Mech. Eng. Sci.* **2021**, *235*, 3792. [\[Crossref\]](#)
- [5] Willumeit, R.; Schuster, A.; Iliev, P.; Lincer, S.; Feuebend, F. *J. Mat. Sci. Mat. Med.* **2007**, *18*, 367. [\[Crossref\]](#)
- [6] Behera, D. R.; Nayak, P.; Rautray, T. R.; J. *King. Saud. Univ. Sci.* **2020**, *32*, 848. [\[Crossref\]](#)
- [7] Pressl, D.; Teichert, C.; Hlawacek, G.; Clemens, H.; Iliev, P. P.; Schuster, A.; Feyerabend, F.; Willumeit, R. *Adv. Eng. Mater.* **2008**, *10*, B47. [\[Crossref\]](#)
- [8] Luthringer, B. J. C.; Katha, U. M. R.; Willumeit, R. *J. Mat. Sci. Mat. Med.* **2014**, *25*, 2561. [\[Crossref\]](#)
- [9] Kochanowski, A.; Hoene, A.; Patrzyk, M.; Walschus, U.; Finke, B.; Luthringer, B.; Feyerabend, F.; Willumeit, R.; Lucke, S.; Schlosser, M. *J. Mater. Sci. Mat. Med.* **2011**, *22*, 1015. [\[Crossref\]](#)
- [10] Nascimento, J. P. L.; Ferreira, M. O. A.; Gelamo, R. V.; Scarmínio, J.; Steffen, T. T.; da Silva, B. P.; Aoki, I. V.; dos Santos Jr, A. D.; de Castro, V. V.; Malfatti, C. F.;

- Moreto, J. A. *Surf. Coat. Techn.* **2021**, *428*, 127854. [\[Crossref\]](#)
- [11] Afzali, P.; Ghomashchi, R.; Oskouei, R. H. *Metals (Basel)* **2019**, *9*, 878. [\[Crossref\]](#)
- [12] Liu, Q.; Liu, H.; Xie, J.; Zhang, W.; Zhang, Y.; Feng, C.; Li, G.; Yu, Y.; Song, S.; Yin, C. *Sci. Rep.* **2022**, *12*, 16586. [\[Crossref\]](#)
- [13] Moreto, J. A.; Marino, C. E. B.; Bose Filho, W. W.; Rocha, L. A.; Fernandes, J. C. S. *Cor. Sci.* **2014**, *84*, 30. [\[Crossref\]](#)
- [14] Kerner, Z.; Pajkossy, T. *J. Electr. Chem.* **1998**, *448*, 139. [\[Crossref\]](#)
- [15] Nelson, A. *J. Electr. Chem.* **2007**, *601*, 83. [\[Crossref\]](#)
- [16] Protopapa, E.; Ringstad, L.; Aggeli, A.; Nelson, A. *Electr. Acta* **2010**, *55*, 3368. [\[Crossref\]](#)
- [17] Gassa, L. M.; Vallejo, A. E.; Alonso-Romanowski, S.; Vilche, J. R. *Bioelectroche. and Bioener.* **1997**, *42*, 187. [\[Crossref\]](#)
- [18] Khalafalla, M. A. H.; Belgacem, C. H.; Ismail, I. A.; Chaieb, K. *J. Electro. Chem.* **2021**, *898*, 115637. [\[Crossref\]](#)
- [19] Bigay, J.; Antony, B. *Dev. cell* **2012**, *23*, 886. [\[Crossref\]](#)
- [20] Moreto, J. A.; Gelamo, R. V.; do Nascimento, J. P. L.; Taryba, M.; Fernandes, J. C. S. *App. Surf. Sci.* **2021**, *556*, 149750. [\[Crossref\]](#)
- [21] Orazem, M. E.; Tribollet, B. *Electrochemical Impedance Spectroscopy*, John Wiley & Sons Ltd, Hoboken, 2008. [\[Crossref\]](#)
- [22] Ohtsuka, T.; Otsuki, T. *Corr. Sci.* **1998**, *40*, 951. [\[Crossref\]](#)
- [23] Okasaki, Y.; Gotoh, E. *Biomat.* **2005**, *26*, 11. [\[Crossref\]](#)
- [24] Alves, A. C.; Wenger, F.; Ponthiaux, P.; Celis, J. P.; Pinto, A. M.; Rocha, L. A.; Fernandes, J. C. S. *Electro. Acta* **2017**, *234*, 16. [\[Crossref\]](#)
- [25] Sivakumar, B.; Kumar, S.; Sankara Narayanan, T. S. N. *Wear* **2011**, *270*, 317. [\[Crossref\]](#)

How to cite this article

Do Nascimento, J. P. L.; Ferreira, M. O. A.; Teixeira, G. T. L.; Leite, N. B.; Aoki, I. V.; Moreto, J. A. *Orbital: Electron. J. Chem.* **2024**, *16*, 10. DOI: <http://dx.doi.org/10.17807/orbital.v15i5.19304>